JAMES RENNELL CENTRE FOR OCEAN CIRCULATION

INTERNAL DOCUMENT No. 3

Wind stress and its dependence on wind speed and sea state

M J Yelland

1992

ABSTRACT

The aim of the project is to detect and quantify the effect of sea state on the wind stress. An overview of the basic theory of wind stress in the surface layer is provided, along with a more detailed description of the inertial dissipation method which is used to obtain stress estimates for this study. Wind stress measurements by other researchers illustrate the large scatter which seems to be inherent in the drag coefficient/wind speed relationship, and parameterisations of the wave field have been suggested to explain at least some of this scatter. Past appraisals of the dissipation technique show it to be capable of measuring wind stress over the oceans. Details are given of the data collection and processing to date. The analysis of the data has so far resulted in an IOS report on the performance of a prototype sonic anemometer, and a paper presenting preliminary results at the 1991 IUGG. Drag coefficients from an early data set are higher than expected and possible reasons for this are discussed. The next stages of data analysis are discussed, and ways of achieving our overall aim of detecting the effect of sea state on wind stress are described.

CONTENTS

1 INTRODUCTION

1.1 Statement of the Problem

Wind stress is a measure of the vertical transport of horizontal momentum in the surface layer (lowest 50 m) of the atmosphere. When momentum from the atmosphere enters the sea, waves, drift currents and turbulence are generated. The sea surface roughness which is caused in this way acts in its turn to affect the wind stress. Hence wind stress is regarded as one of the key parameters in air-sea interaction.

Oceanographers need to know the wind stress to determine the atmospheric forcing of the ocean's circulation, and meteorologists use it as a lower boundary condition. Improved estimates of the air-sea exchange rates are produced when the mixed layers of the ocean and atmosphere are modeled as a coupled system, and a better understanding of the flux processes are needed to do this. Climatologists are also interested in the stress-related exchange rates and fluxes (e.g. of CO_2) through the sea surface. Wave height, aerosol generation and whitecap coverage all scale with the wind stress, and the growth and spectra of surface waves are determined by it. The return signal received by scatterometers (such as that on board ERS1) depends on wind stress and can be used to infer the wind field over the oceans if the wind stress / wind speed relationship can be determined.

Many researchers have tried to determine this dependence of wind stress on wind speed, with the eventual agreement amongst the majority that the stress increases with wind speed. However, there is a large amount of scatter in the data collected to date, no consensus on an exact relationship, and many different suggestions as to other possible parameters which need to be measured to improve the relationship (see section 2). Our aim is to decide on the simplest set of variables which can be used by us to determine the drag coefficient in a routine fashion, using data from the Voluntary Observing Ships say.

This work is directly relevant to the IOS programs for WOCE (which has a goal to reduce errors in stress estimates to 20% at most), upper ocean processes (to improve the modelling of the forcing terms in mixed layer

models), and the ERS1 scatterometer (to implement a routine method of stress measurement suitable for scatterometer calibration/validation while quantifying the stress/wind speed relationship).

The next section of the introduction will cover the basic theory behind the parameterisation of wind stress, and section 1.3 describes the methods commonly used to calculate it.

Section 2 describes the background to the research in this area, beginning in section 2.1 which reviews previous stress measurements. Section 2.2 describes previous comparisons between two different methods of estimating wind stress; the eddy correlation method (often regarded as the standard), and the inertial dissipation method, since this latter technique is the one chosen for the collection of our data. Section 2.3 is a brief review of papers on the effects of sea state on wind stress.

The work undertaken for this study.is presented in section 3. It is introduced by the plan of our research to date in section 3.1. The collection of our data is described in section 3.2 and the analysis and results are described in sections 3.3 and 3.4 respectively. Finally, the plan of the work to be undertaken over the next three years is described in section 3.5.

1.2 Theory

In the lowest 50 m or so of the surface layer of the atmosphere (depending on stability), the wind stress, τ, is regarded as being independent of height. Wind stress is defined as;

$$\tau = -\rho <uw> \tag{1}$$

where the brackets denote a time average of u and w; the along wind and vertical wind speed fluctuations.

In this layer, a friction velocity, $u*$, may be defined by;

$$u*^2 = \tau / \rho \tag{2}$$

where ρ represents the density of air. Wind stress can then be related to wind speed relative to the sea surface, U, through two parameterisations.

One is via the drag coefficient, CD;

$$u*^2 = CD\ U^2 \tag{3}$$

which is known as the bulk aerodynamic formula.

The other is via the roughness length, z_0, and is derived from mixing length theory (Stull, 1988). For neutral conditions;

$$dU/dz = u_* / k_v z$$

which, when integrated from a height z_0 (where $U = 0$), becomes;

$$U / u_* = \ln (z/z_0) / k_v \qquad (4)$$

where k_v is the von Karman constant, and z is the measurement height above the sea surface.

Hence wind stress can be determined from wind speed if either the drag or roughness are known, and drag and roughness can be found from each other;

$$CD_N = (k_v / \ln(z/z_0))^2 \qquad (5)$$

Where the subscript N refers to neutrally stratified conditions.

At present, a simple relationship is often used to predict the drag coefficient directly from wind speed. It takes the form;

$$CD \ 10^3 = a + b \ U \qquad (6)$$

or $\qquad CD_{10N} \ 10^3 = a + b \ U_{10N}$

where the subscript 10 represents a reference height of 10 m above sea level.

Wind stress results are therefore generally displayed as a plot of drag coefficient vs. wind speed. The constants a and b take different values depending on the conditions prevailing at the site where the data was collected, and individual data sets contain a great deal of scatter. It is generally accepted that this implies the possible presence of other variables, most notably that of sea state, which could influence the determination of the drag coefficient. The problem then becomes one of determining the dependence of the drag (or the roughness length) on these other variables.

For example, Charnock (1955) proposed a relationship between friction velocity and roughness length, which was based on simple dimensional constraints;

$$z_0 = \alpha \ u_*^2 / g \qquad (7)$$

where α became known as the "Charnock constant". In this case, the effects of sea state are hidden in the "constant".

1.3 Stress Measurement Methods

The next section briefly describes the main methods of estimating wind stress. In general, either the wind speed and/or the turbulence of the atmosphere are measured and converted into wind stress or friction velocity estimates.

The **bulk method** relies on equation (3) with an *assumed* mean drag coefficient estimated from equation (6). Hence wind stress estimates can be produced from wind speed measurements, but with a large uncertainty in the mean value, and a large scatter. This method is unable to detect any changes in the sea-state or other variables in which we are interested, and is only useful for long term (few days or more) averages of the stress.

The **wind profile method** is one of the older methods of measuring wind stress. For this method, wind speed is measured at three or more heights simultaneously and equation (4) is used to calculate the friction velocity and roughness length. This method requires very accurate wind speed measurements, and is very sensitive to distortion of the wind profile. These problems, and the variable nature of z_0 over the ocean, make it difficult to produce accurate stress measurements from this method.

The most popular method in more recent years has been the **eddy correlation** (or "direct covariance") technique. This involves measuring all three components of the wind speed and calculating the wind stress directly from equation (1). The eddy correlation method is normally considered the standard in that it provides a direct measurement of the desired time-averaged covariance at the measurement height. However, since equation (1) must be integrated over a wide range of frequencies this method is sensitive to flow distortion, and sampling times of more than ~30 minutes are needed. It is also extremely difficult to use on moving platforms such as ships and buoys since the platform motion has to be measured in order to remove it from the wind measurements. Great accuracy is needed in the measurements since the vertical wind speed signal is very small. The necessity of a stable platform restricts this technique to relatively shallow water coastal sites, which accounts for the lack of data collected in deep water, open ocean sites.

The last method to be considered here is that of the **dissipation technique**, or, more precisely, the "inertial dissipation technique". This will

be discussed in more detail since it is the method used for our data collection. In this case, a time series of wind speed is recorded over 10 minutes or more, and a spectrum produced using an FFT (Fast Fourier Transform). Turbulent kinetic energy (TKE) is generated at the lower frequency end of the spectrum and is dissipated by viscous damping at the highest frequencies. For steady-state turbulent flow, the energy cascades down from lower to higher frequencies and, in a certain range, this flow of energy is governed entirely by the rate of energy dissipation, ε, at the high frequency end. The turbulence over this range of frequencies (called the "inertial subrange") must be isotropic. Using dimensional analysis, the power spectral density, S, can be related to the dissipation rate via the wavenumber, n;

$$S(k) = K \, \varepsilon^{2/3} \, n^{-5/3} \qquad (8)$$

where K is the Kolmogorov constant. Using Taylor's hypothesis, i.e. assuming "frozen" turbulence, this becomes;

$$S(f) = K \, \varepsilon^{2/3} \, f^{-5/3} \, (U_r / 2 \, \pi)^{2/3} \qquad (9)$$

where U_r is the relative wind velocity. Hence, in the inertial subrange, the spectra has a -5/3 tail, and the dissipation rate can be easily obtained from the power spectral density. Figure 1 shows spectra which have been normalised by multiplying the spectral density by $f^{5/3}$ to produce a flat region over the inertial subrange. To find the friction velocity, divergence and storage of turbulent kinetic energy are assumed zero, and the dimensionless dissipation function is used;

$$k_v \, \varepsilon \, z / u_*^3 = \Phi \qquad (10)$$

where z is the reference height and Φ is a function of stability which equals unity for neutral conditions. The stability functions have been investigated extensively over land, and some of the results have been verified over the oceans (e.g. Geernaert, 1990). For example, those of Dyer (1974) were verified for use over the oceans by Smith (1980);

$$\Phi = 1 + 5z/L \qquad z/L > 0 \qquad (11)$$
$$\Phi = [1 - 16z/L]^{-1/4} \qquad z/L < 0$$

where L is the Monin-Obukhov length;

$$L = -T \, u_*^3 / g \, k_v <t \, w> \qquad (12)$$

where k_v is the von Karman constant, T is the absolute air temperature, t is the virtual temperature fluctuation, and w is the vertical wind fluctuation. For our data, the buoyancy term ($<t \, w>$) was estimated from bulk formulae.

For the dissipation method to apply, certain assumptions must be made. These are;

1) assumption of local isotropy

2) the validity of the Monin-Obukhov scaling parameters

3) negligible local source, sink, and transport terms of TKE (although Large and Pond (1981) verified that the transport terms were indeed negligible, and were satisfied that equation (10) was valid).

Overall, the dissipation method is a good compromise, being less sensitive to low frequency platform motions than the eddy correlation method, and less sensitive to platform distortion of the air flow than the eddy or the profile methods since it uses only the high frequency part of the spectrum (section 2.2). It is a more direct method than the bulk because it is a true turbulence statistic.

Whichever method is chosen to make the stress measurement, the problem remains of accurately determining the wind speed before the drag coefficient can be calculated. For a stationary platform such as a tower, currents need to be measured since the true wind is defined as air flow relative to the water surface. If, on the other hand, wind speed is calculated relative to the ground for convenience, then the problem of logging a ship's motion is encountered. Most importantly, the results are not equivalent and can not be compared.

2 HISTORIC BACKGROUND

2.1 Previous Stress Measurements

Measurements of wind stress parameters have been performed, according to Roll (1965), since at least 1875 when Colding estimated the drag coefficient to be $2.6*10^{-3}$ under strong wind conditions (> 10 m/s). Early methods of estimating the drag coefficient reviewed by Roll included;

1) Sea surface tilt method; used on stationary, enclosed bodies of water, where the tilt of the surface due to wind action had to be measured to 1cm in 100km. Used by Colding in 1875.

2) Geostrophic departure method; the departure from the geostrophic wind throughout the atmospheric boundary layer is measured to

determine the mean stress on a scale of 10 to 100s of km. First applied to the friction layer over the oceans by Sutcliffe in 1936.

3) Wind profile method; wind speed measurements are taken simultaneously at different heights above the sea surface. Used by Shoulejkin in 1928.

4) Eddy correlation; measurements taken of the horizontal and vertical wind speed fluctuations from the mean. This technique was first used over the oceans by McIlroy in 1955.

Roll also describes the review performed by Wilson in 1960, which summarised forty-seven drag coefficient measurements obtained by these various methods, and concluded that;

$$CD_{10} = 2.37 \ (\pm \ 0.56) \ 10^{-3} \quad U > 10 \text{ m/s}$$

$$CD_{10} = 1.49 \ (\pm \ 0.83) \ 10^{-3} \quad U < 10 \text{ m/s}$$

Garratt (1977) reviewed drag coefficient measurements performed during the late 1960s and early 1970s, most of which used either the eddy correlation or the wind profile methods. Some of the data showed no dependence of the drag on wind speed, but overall this review resulted in a drag coefficient/wind speed relationship of;

$$CD_{10N} = 0.75 + 0.0647 \ U_{10N}$$

which is indicated in Figure 2 by a dotted line. Garratt attributed most of the systematic differences between the data sets, and the scatter in individual data, to calibration uncertainties in the sensors. In addition to calibration errors, insufficient averaging times (10-30 minutes rather than the 30-60 minutes recommended for the eddy correlation method as a result of studies by Miyake et al. (1971) and Tsvang et al. (1973)) were expected to produce a scatter of 10-15%. This experimental scatter obscured any effect which may have been due to fetch or wind duration or unsteadiness, and most data sets did not include any information on these variables.

More recently, Geernaert (1990) reviewed 10 drag coefficient/wind speed relationships determined during the previous twenty years. This review, unlike Garratt's, included data obtained using the dissipation method as well as that from the more conventional eddy correlation and wind profile methods. Geernaert's summary is reproduced in Table 1 below.

Table 1

SPEED m/s	$CD_{10N} = $ 10^3	% SCAT	Nº SAMPLES	METHOD	PLATFORM, LOCATION	DEPTH m	REFERENCE
5-25	0.58+0.085u	20	116	Eddy Correlation	tower, North sea	30	1
5-21	0.43+0.097u	12	186	Eddy Correlation	mast, North sea	15	2
	0.20+0.117U	(as above, with corrections for surface currents)					2
7-17	1.09+0.094u	-	145	Wind profile	mast, lake Geneva	3	3
4-17	0.37+0.137u	28	120	Eddy Correlation	tower, lake Ontario	10	4
5-19	0.46+0.069u	28	120	Eddy Correlation	BIO tower, Atlantic	DEEP	5
4-10	1.14	16	590	Dissipation	tower / ship, open ocean	DEEP	5
10-26	0.44+0.063u	16	1001	Dissipation	tower / ship, open ocean	DEEP	5
6-22	0.61+0.063u	25	120	Eddy Correlation	BIO tower, Atlantic	DEEP	6
2.5-21	0.63+0.066u	30	111	Eddy Correlation	mast, Atlantic	DEEP	7
4-18	1.29+0.03u	17	70	Dissipation	ship, open ocean	DEEP	8
2.5-16	.36+.10u	20	233	Wind profile	tower, Lough Neagh	15	9

1 Geernaert *et.al.*(1987), 2 Geernaert *et.al.*(1986), 3 Graf *et.al.*(1984)

4 Donelan (1982),   5 Large, Pond (1981),   6 Smith (1980)

7 Smith, Banke (1975), 8 Denman, Miyake (1973), 9 Sheppard *et.al.*(1972)

Figure 2 shows these relationships summarised by Geernaert (1990) by solid lines labelled with the reference number from Table 1.

These data all show an increase in drag coefficient with wind speed but the rate at which it increases varies between data sets, so, for a given wind speed, the predicted drag coefficient will vary. Much of this variation is assumed to be due to sea state, with deep water sites generally providing lower drag coefficients than shallow water sites. The results of Large and Pond (1981) and Smith (1980) are some of the lowest and are often taken as being representative of deep water, open ocean conditions.

Also evident is the scarcity of data obtained at wind speeds above 20m/s, and the absence of data above 26 m/s. Smith observes that, although these higher wind speeds account for only a very small fraction of the long term (monthly or more) mean stress, they are important in modelling such events as storm surges. At present, the only estimates for drag under high wind speed conditions have been obtained by the geostrophic departure method Roll (1965).

To summarise, measurements of sea surface drag are inherently scattered, typically by ~20% or more. The mean differences between data sets and the scatter within them can be attributed to variables such as sea state, depth, fetch or slicks, but other causes of scatter need also to be considered. Smith (1980), suggests that changes of less than 20% in drag coefficient may be difficult to resolve because of A) experimental errors in sensor response B) flow distortion by, and motion of, the support tower, and C) the use of a finite averaging period to represent long term, steady state conditions. This figure will be increased unless great care is taken in both defining and calculating true wind speed. In most of the research discussed above there is little or no mention of current measurements, so it is assumed that the wind speeds were all calculated relative to the ground. Hence, possible currents could be partly responsible for both scatter and mean differences in the drag coefficient results. The one exception is Geernaert et al. (1986) who, after correcting his results for surface currents, found that the calculated drag coefficient decreased by ~5% at a wind speed of 10 m/s.

2.2 Dissipation Technique - Comparisons with Eddy Correlation Method

Schmitt et al. (1978) reports Gibson and Williams as the first to use the dissipation technique (neglecting stability effects) over the open ocean in 1969. Schmitt performed a comparison of stress measurements obtained via the eddy correlation and the inertial dissipation methods. A sonic anemometer was mounted 8m above sea level on a tower in 20 m of water, and levelled to within 0.1 degree. Six runs were obtained, between 20 and 60 minutes in duration, where the wind speed was steady (6m/s $\pm$ 1) and of a constant direction. Bulk formulae were used to estimate stability. No mention is made of current measurements. The results from the dissipation method showed a

drag coefficient 30% higher on average than that found by the eddy correlation method ($CD = (0.99 \pm 0.37)10^{-3}$ for the former and $CD = (0.77 \pm 0.10)10^{-3}$ for the later). However, the considerable scatter in both sets of results reduces the significance of the mean difference. Schmitt also found evidence for local anisotropy in the ratio of the vertical to streamwise velocity spectra in the inertial region. This ratio should be 4/3 under isotropic conditions, whereas a ratio of 1.06 was found on average for his data. He showed this was not due to buoyancy forces since the streamwise and perpendicular spectral ratio also departed from that expected under isotropy. The same anemometer was used in a similar experiment over land and produced spectral ratios consistent with isotropic conditions, thus eliminating instrument error. Schmitt suggested that anisotropy will be greater nearer to the surface and will depend on the wave height to measurement height ratio, with the suggestion that anisotropic effects will be significant at ratios less than 5-10. He recommended measuring the pressure field as well as the wave field.

Large and Pond (1981) obtained a much larger data set (192 runs of 40 or 60 minutes) which covered a wind speed range of 4 to 20 m/s. A propeller anemometer was used, mounted 12.5m above mean sea level on a Bedford Institute tower situated in deep (59 m) water, with fetches of at least 10km. Stability corrections were calculated using Dyer's (1974) stability functions and measurements of wind speed, air temperature and sea temperature (10 m below sea level). Air pressure was obtained from a land based meteorological station 15 km north of the tower. No measurements of surface currents are mentioned. Results obtained from the eddy correlation method were;

$$CD_N \ 10^{-3} = 0.46 + 0.069 \ U_{10}$$

or

$$CD \ 10^{-3} = 0.43 + 0.069 \ U_{10}$$

which agrees excellently with that found independently, but at the same time and site, by Smith (1980);

$$CD \ 10^{-3} = 0.44 + 0.063 \ U_{10}$$

When drag coefficients were calculated using the dissipation method with stability corrections, the results agree within 4% with those from the eddy correlation method except for the most stable cases. For very stable cases ($z/L > 0.1$), the dissipation method produced fluxes that were 5-10% higher

than those from the eddy correlation, but such conditions are infrequent over the oceans.

Having proved the dissipation method to the authors' satisfaction, the data set was extended. 1086 hours of dissipation data was obtained on the tower, in addition to 505 hours obtained on the weather ship Quadra which carried an anemometer 22m above sea level. For most of the time the ship steamed into the wind at less than 4 knots, and the true wind speed was found by correcting the measured wind speed vectorially for the ship's speed over the ground as determined from the ship's position (given by satellite fixes). After rejecting spectra that did not conform within 10% to a -5/3 slope, this data produced;

$$10^3 CD_N = 1.14 \qquad \text{for } U_{10} < 10 \text{m/s}$$
$$10^3 CD_N = 0.49 + 0.065 U10 \qquad \text{for } 10 < U_{10} < 26 \text{m/s}$$

Apart from an overall agreement with the eddy correlation results, the extended dissipation data set showed that the stability corrections used were satisfactory, at least for $z/L < 0.15$. There was evidence to suggest that the drag coefficient was independent of fetch for fetch/z > 800, and that it increased for increasing winds. Most importantly, for our purposes, the results showed that the dissipation method produces reliable wind stress measurements when used on a moving platform.

Additional data from the ship CCS Parizeau 1980 cruise (Large and Pond, 1982) agreed with the above results.

During the FASINEX experiment Large and Businger (1988) collected 162 hours of stress measurements using the dissipation technique, for a wind speed range of 3-10 m/s. Two propeller anemometers were mounted on the RV Endeavor, 10m and 13.5m above sea level, and the measured wind speeds were corrected by calculating ship speed from the ship's satellite navigation and LORAN systems. The error in true wind produced by this method was estimated to be about 10%, and could be as great as a few m/s, which will have introduced large errors in the estimates of drag coefficient. However, an accuracy of 10% in u_* was seen as achievable and the results agreed with that from the researchers' previous studies. Statistically steady results were achieved from sampling periods of 20 minutes. When compared with results from the bulk method, the dissipation wind stress agreed over periods of days, but was found to differ by a factor of 2 over periods of a few hours, attributed to possible changes in z_0 to which the bulk

method can not respond (section 1.3).

During the 3 day TOWARD experiment 2km off the Californian coast, Geernaert et al. (1988) compared 30 minute averages of wind stress from the dissipation technique (using a hot film instrument) and the eddy correlation technique (using a sonic anemometer) for wind speeds of less than 9m/s. Both instruments were mounted on a tower at a height of 22m above sea level. The water depth of 15m was considered "deep" for wind waves, but swell were treated as being steep, shallow water, waves. The results of this comparison showed that the two techniques agreed well under near neutral conditions, but for stable conditions (and especially during non-stationary conditions) the dissipation method underestimated the stress by up to 40%. This disagreement of results suggested that the stability corrections, pressure transport term and energy divergence may all need more investigation.

However, in a later paper, Geernaert (1990) confirms that, for near neutral and unstable conditions, the imbalance term in the TKE budget is negligible, and that the expression;

$$u_*^3 = k_v \, z \, e \, / \, \Phi$$

(equation (10) above) is valid. For this study, Kaimal's stability terms were used;

$$(1+0.5|z/L|^{3/5})^{-3/2} \quad \text{for } z/L<0 \qquad (13)$$
$$(1+2.5(z/L)^{2/3})^{-3/2} \quad \text{for } z/L>0$$

The most recent, and most exhaustive, comparison of the dissipation and eddy correlation techniques was performed during the HEXOS experiment in the autumn of 1986. The Meetpost Noordwijk platform, standing in deep (20 m) water off the Dutch coast in the North Sea, was used. Edson et al. (1991) presented the results from the stress comparisons obtained, under near neutral or slightly unstable conditions, during the HEXOS main experiment (HEXMAX). Two packages of anemometers were deployed, each containing sonic anemometers and hot wire or film anemometers; one package was on a boom extending out from the platform at a height of 5-8 m above sea level, and the other was on a mast on the platform, at a height of 26m above mean sea level. The site of the instruments on the mast experienced flow distortion, and was chosen intentionally so that the effects of flow distortion on the measured fluxes could be studied. Ten minute means of

the wind stress were computed and averaged into 50 minute values.   The mean vertical and crosswind components were forced to zero to allow for instrument tilt.

The results showed that the wind stress from the dissipation and eddy correlation methods agreed very well (Figure 3), and that in areas of flow distortion, the dissipation method was much less affected than the eddy correlation.   Assuming a balance between the production and dissipation of TKE, the Kolmogorov constant was found to be 0.55 ± 0.01, which agrees with that used by Large and Pond (1981), and is the value used for our data.

In summary, the dissipation method performs well in the near neutral or unstable conditions which predominate over the oceans, and has distinct advantages over the eddy correlation method where platform motion or wind flow distortion occur.

2.3 The Effect of Sea State on Wind Stress

Some work has previously been done on the effect of wave height on wind stress where the degree of equilibrium between the waves and the wind has been ignored.   For example, Smith (1980) showed an increase in the drag coefficient with wave height for long fetch and near neutral conditions. However, this dependency was less well correlated than that of the drag on the wind speed, and so seems to be of less practical use.   This section will concentrate on work which uses some form of wave age parameter as a measure of sea state.

As mentioned in section 1.2 above, the Charnock "constant", α , like the drag coefficient or the roughness length, is thought to depend on sea state. Stewart (1974) considered that the roughness length,   when non-dimensionalised by the acceleration due to gravity, g, and the friction velocity u_*, could be expressed as a function of wave age. i.e.;

$$g \ z_0 \ / \ u_*{}^2 = f \left(C_p \ / \ u_* \right) = \alpha \tag{14}$$

where C_p is the phase speed of the of the dominant wind wave.   In this case, Charnock's relationship will only be valid for wave and wind fields in equilibrium, i.e. in a fully developed sea.   Denman and Miyake (1973) suggested that this is the reason why values of the Charnock "constant" vary for different data sets.

Masuda and Kusaba (1987) generalised (14) by using;

$$f(C_p / u_*) \propto (\sigma_p u_* / g)^m \tag{15}$$

where σ_p is the angular frequency of the peak wind wave. This becomes Charnock's relationship when $m=0$.

Toba and Koga (1986) proposed, for developing wind waves under a steady wind field, that $m=-1$. i.e.;

$$g z_0 / u_*^2 = \gamma g / \sigma_p u_* \quad \text{or} \quad z_0 \sigma_p / u_* = \gamma \tag{16}$$

where γ is a constant. Later, Toba et al. (1990) applied this relationship to equilibrium wind waves under a strong wind. This implies that as waves get "older" (i.e. C_p / u_* or, equivalently, $g / \sigma_p u_*$ increases) the roughness increases. This is the opposite conclusion to that of many other researchers (e.g. Volkov (1970), Hsu (1974), Donelan (1982), Geernaert et.al. (1987), Masuda and Kusaba (1987), and Janssen (1989)) who find $0<m<1$ both through measurement over the ocean, in wave tanks and from models. Hence the majority opinion is that the roughness decreases with wave age.

Hasse (1986) cast doubts on the usefulness of the Charnock relation. Since the relation ought to apply for neutral conditions, g must appear as a wave field parameter rather than an atmospheric buoyancy parameter. This implies that it is the gravity waves that determine roughness, but typical roughness lengths at sea are $\sim 10^{-4}$ m. This implies a wave height of ~ 0.5 cm and a wavelength of ~ 5 cm, which is rather small for wind driven seas under average wind speeds. These size waves are close enough to the capillary wave size to suggest that surface tension should be an important factor. For these and other reasons, Hasse decided that it is impossible to relate the roughness length to geometric properties of the sea surface in a simple way, and that "the use of the drag coefficient makes it much more evident that we are attempting to summarize a rather complicated process in a single coefficient."

3 PROGRESS TO DATE

3.1 Strategy Adopted

Previous wind stress measurements have been limited by time constraints and sometimes by recording and processing constraints. So, in order to achieve our aim of defining an improved set of variables from which the drag coefficient can be measured, we have adopted two strategies;

i) The first involves the collection of high quality data sets where large numbers of variables are measured as accurately as possible. The collection of such detailed data has been the aim of two of the recent research cruises undertaken on the RRS Charles Darwin; CD43 in November 1989, and CD62a in September 1991. In this way we hope to determine which variables are the most important.

ii) The second, more empirical, method uses a data set of lower quality which has been gathered almost continuously over the past three years. This long-term data set should cover a much wider range of conditions than previous research. This type of data is collected routinely on the weather ship Cumulus. In this case, data will be split into case types according to conditions and the results from each type compared against each other.

Figure 4 is a guide to the summary of data collected and processed to date, described in the following sections.

3.2 Assembly of Data sets

3.2.1 Instruments used

For a high quality data set, such as that obtained during a RRS Charles Darwin cruise, variables which should be measured include; wind speed and direction (relative to the ship), ship speed relative to the water (using an em log) and over the ground (using the ship's GPS system), wind spectra, wave field, surface current (using a VAESAT buoy), wet and dry bulb air

temperatures, sea surface temperature, and air pressure. The temperature and pressure measurements are used to calculate the stability corrections to the basic stress calculation (after Large and Pond (1981)). Only a subset of these measurements are taken routinely on the OWS Cumulus.

The instruments used for wind speed data are:

i) Young propeller-vane anemometer. This is used to produce mean wind speed and direction values averaged over one minute. The output is also sampled at 8Hz to produce 5 minute means of power spectral density (PSD), which have to be corrected for the instrument's poor frequency response. This correction can be rather large, especially at low wind speeds (a factor of ~5 at 5 m/s), so proportionally large errors can be expected.

ii) Solent sonic anemometer. This was a prototype instrument when first used on CD43. It had the advantage of a much faster response than the Young, without the need for large correction factors.

iii) Kaijo-Denki sonic anemometer[*]. Until recently, this was the standard sonic anemometer, and as such was used as a comparison when evaluating the Solent sonic anemometer during CD43.

The instruments used for wave field data are;

i) Ship Borne Wave Recorder (SBWR). This produces one dimensional wave spectra from a 10 or 20 minute sample. This instrument has a poor response to the high frequency end of the spectrum and does not register anything above ~0.3 Hz. The correction for the poor frequency response rises rapidly to a factor of 5 at 0.2 Hz and above. This means that no information can be obtained about the generation, or early stages of growth, of wind waves. Since the spectra are also one dimensional, no directional information is available. The main advantage of the SBWR is that it is on the ship (!), so that the wave field produced corresponds spatially to the wind stress estimates produced by the ship's instrumentation.

ii) Directional wave buoys (a WAVEC on CD43 and a directional Waverider on CD62a). These produce directional spectra of the wave

[*] The Kaijo-Denki sonic anemometer was operated by researchers from the University of Manchester Institute of Science and Technology, who very kindly shared their wind speed and PSD results with us.

field up to about 0.6Hz, which is high enough to resolve all but the generation of wind waves. This data is only useful when wind stress estimates are obtained near the wave buoy, which requires the ship to be within a few kilometres at most.

3.2.2 RRS Charles Darwin cruises

A five week research cruise (CD43) took place to the Faeroes region of the North Atlantic during October and November of 1989. Various meteorological instruments were deployed on the ship itself. Those used in this work were a prototype Solent sonic anemometer, a Young propeller anemometer and a Kaijo-Denki anemometer, all of which were mounted on the foremast of the ship, as were the psychrometers. Except when steaming between CTD stations, the ship was hove-to head to wind so as to provide an undisturbed air flow over the instruments on the foremast. The Charles Darwin is fitted with a Ship Borne Wave Recorder (SBWR), which provided (non-directional) wave spectra throughout the cruise.

In addition to the instruments on the ship, data was obtained from a WAVEC directional wave buoy and a VAESAT current measuring buoy. The WAVEC buoy transmitted data to a shore station on the Faeroe Islands, and to the ship when it was within range. This system worked well except for a ten day period during the middle of the cruise, when no data was received at the shore station and the ship was out of range. When the ship was relatively close to the buoys, the data obtained from them could be used to upgrade the wave field information.

During September 1991 the Charles Darwin returned to the Faeroes region of the North sea on a three week ERS1 validation cruise (CD62a). One of the subsidiary aims of the cruise was to obtain a high quality data set containing continuous wind stress estimates and directional wave data. This was to be obtained by deploying a directional Waverider buoy along side a new buoy which carried meteorological instruments, including a Solent sonic anemometer. Unfortunately, the Waverider buoy was believed to have been run down by a trawler before the new meteorological buoy could be deployed, so concurrent data sets were not obtained. In addition, the meteorological buoy capsized less than a day after deployment; however, enough data was produced for an initial evaluation of the system.

As in CD43, the Darwin was fitted with a SBWR and carried

meteorological instruments on the foremast. In this case, a Young propeller anemometer and two Solent sonic anemometers were used. Unlike the prototype used during CD43, these Solent sonics were production models which incorporated new features, such as an increased sampling frequency (transducers fired at 168 Hz compared to 42 Hz for the prototype, with less possibility of aliasing). A new version of the Solent sonic with a different sensor head arrangement was also tested.

3.2.3 OWS Cumulus

The weather ship Cumulus has been on station Lima (57°N 20°W) since the early 1970s. The station area covers a 10km square, where the ship is allowed to drift (beam onto the wind) until it approaches the boundary of the area, at which point it steams back across the area and repeats the process, for about four weeks in five. The ship was fitted with a SBWR during 1985, and, since November 1988, has been carrying a fast sampling system based on a Young propeller anemometer, capable of producing wind stress estimates. There are good measurements of wet and dry bulb air temperature, but for pressure, sea surface temperature and swell direction the only information comes from the three-hourly Met. Office observations carried out by the ship's crew. There is also no information about ship's speed through the water, and ship's position is only recorded hourly. When the ship is steaming it is safe to assume that the ship's direction and the ship's head are very nearly the same, but when the ship is drifting there is no very reliable information as to the ship's head.

3.3 Processing and Analysis of Data

3.3.1 RRS Charles Darwin

3.3.1.a) Wind speed and stress data

An extensive analysis of the prototype Solent sonic anemometer was carried out by comparing its performance to that of the two other anemometers on the foremast. The results were published in an IOS internal report Yelland et al. (1991). In brief, the Solent sonic performed well throughout CD43,

and produced wind speed and wind stress estimates in agreement with those from the other anemometers. Figure 5 shows the wind speed values from the Solent against those from the Kaijo-Denki, and Figure 6 shows a comparison of the friction velocities.

During the three weeks of CD62a, the Young anemometer was positioned on the port side of the foremast platform, and the two Solent sonic anemometers occupied sites on the starboard side of the platform. Initially, the two sonics were side by side, both upright and at the same height (15.7m above sea level). This direct comparison showed the wind speeds recorded by the two sonics to be in excellent agreement (Figure 7). After 7 days, the inboard sonic (serial nº 10) was inverted so that the sensor head was at a height of 12m, in an attempt to test whether the logarithmic wind profile relationship was valid. Eight days later the positions of the sonics were exchanged so that the sonic(10) was in the upright outer position and the other sonic(11) was now inverted in the inboard position. We hoped this would enable us to separate the signal due to differences in the anemometers' performance from that due to the anemometers' height difference. Unfortunately, the vertical wind speeds were not recorded and so we were unable to measure any mean vertical tilt of the instruments. For a logarithmic wind profile, the ratio of the wind speeds at heights of 12m and 15.7m should be;

$$U_{12} / U_{15.7} = 0.9775$$

i.e. a 2.25% difference. But a mean tilt of 4 degrees from the vertical would produce a decrease in the measured wind speed of 0.25%. This means that apparent slight deviations from the expected wind profile can not be relied upon, since they may be caused by instrument tilt.

The Solent sonic used on CD43 had a symmetric arrangement of three support struts around the sensor volume, as did the two sonics used for most of CD62a. An alternative version of the Solent sonic with an asymmetric head arrangement was also used towards the end of CD62a, in order to evaluate the hoped-for improvement in spectral estimates that the new head arrangement was designed to produce. For the last few days of CD62a the inboard sonic was replaced by one with an asymmetric arrangement of support struts, in the upright position, in order to compare it directly with the outer symmetric sonic. This data has yet to be processed.

3.3.1.b) Wave data

The SBWR data needed little processing to produce wave heights and spectra. The directional Wavec data from CD43 was processed as described by Ewing (1986).

Figure 8 shows a time series of the spectra obtained from the SBWR. Figure 9 shows a comparison between significant wave height (Hs) from the SBWR and the Wavec, which illustrates a reasonable behaviour from the SBWR. Since all data is shown here, including when the ship and the buoy were 100 Km or so apart, some scatter is to be expected.

3.3.2 OWS Cumulus

3.3.2.a) Wind speed and stress data

Raw wind speed and stress data from Cumulus are available from November 1988 up to the present. The first problem to be solved was the major question of correcting wind speed measurements for ship speed. Since their is no em log information available for the Cumulus, ship speed relative to ground was calculated from the ships position, recorded hourly in the Meteorological Observations log. A program has been written to treat the recorded wind speeds according to whether the ship is judged to be steaming or drifting (beam on to the wind). Since the ship's position is known only once an hour, and the ship's head is unknown while it is drifting, certain assumptions have to be made before the data can be corrected. However, the situation will be improved in January 1992 by the installation of a GPS (Global Positioning System), which will give ships position and head every minute.

No wind spectra have been processed yet.

3.3.2.b) Wave data

Some SBWR data from the Cumulus has been processed to produce spectra like those in section 3.3.1b. The processing of SBWR data from the Cumulus was not as simple as that from the Darwin because of the way the raw data was recorded. The SBWR on the Darwin produced raw spectral data every 20 minutes, whereas on the Cumulus the data was split into two

ten minute halves. All the first ten minute spectra from each 20 minute period were recorded to one file, and all the second spectra were recorded to a separate file. This was done to minimise the risk of losing data, since the ship's routine radio transmissions had caused troublesome electrical interference. A program was written to sort, order and check the spectra for signs of interference before continuing with the usual processing.

3.4 Results

The processing and analysis of data from CD62a and Cumulus are incomplete so this section will concentrate on the results from the first RRS Charles Darwin cruise, CD43.

3.4.1 Mean drag coefficients

Figure 10 shows the drag coefficient values against wind speed (after adjusting both to 10m height and neutral conditions), for each of the anemometers. Also shown is the Smith (1980) relationship, which is normally taken as representative of the deep ocean, long fetch conditions which prevailed during cruise CD43. It is clear that the drag coefficients obtained during CD43 are significantly higher than those of Smith, but it is not presently known whether this is due to the airflow rising over the bow of the Darwin, the method used to calculate wind speed (a correction was applied to the CD43 data to allow for the ship's speed through the water, as measured by the em log), or a combination of these factors. This discrepancy was part of the motivation for CD62a where ship data could be compared to that obtained from the buoy.

Figure 11 shows drag coefficient against wind speed for the Solent sonic only. Here, wind speed has been corrected for ship speed in two ways; using the em log (solid line) and using ship speed calculated from the ship's position (dashes). It can be seen that the two correction methods produce very similar mean drag coefficients. However, the two correction methods have different errors inherent in them. The method using the ship's em log could be affected by the use of the bow thruster which ejects a stream of water in a variable direction in order to improve the handling of the ship at low speeds. This stream of water passes under the ship, and in certain orientations the flow of water will pass the em log sensors, causing an

erroneous reading. Unfortunately, it is not known how often or in what manner the bow thruster was used. On the other hand, the use of the ship's position to calculate ship's speed assumes that there are no currents present. Use of the VAESAT current buoy data has shown that the current has a tidal component and generally varies between 0.6 and 1 m/s. Further work with this data may improve the wind speed corrections.

In addition to the problems we experience in calculating a true wind, a parallel problem occurs when comparing our results with those from other researchers. For example, Smith (1980) makes no mention of any measurements of currents in the area of the BIO tower, and the only corrections Large and Pond (1981) apply to their data from the same area is to remove ship speed over the ground. So if a steady current was prevailing in the area of their research, or in ours, it is impossible to draw conclusions about mean differences in the calculated drag coefficient.

A more serious problem arises when the effect of waves on wind stress is being considered. This is because sea state is expected to be responsible, at least in part, for the scatter in the measured drag coefficient. Therefore, if there are varying currents which are not measured, or if the use of the em log is affected in an unknown and varying amount by the use of a bow thruster, then the scatter in the drag coefficient which is due to sea state may well be masked by scatter introduced in the wind speed calculation. Figure 12 illustrates this problem. It shows a scatter plot of drag coefficient from the Solent sonic anemometer using the two different correction schemes. The same data is used and is processed in an identical fashion. The only difference is in the method of correction for wind speed, so the scatter in this plot, of the order of 20%, is due entirely to the methods of calculating true wind speed.

3.4.2 Wave age effects - IUGG Vienna

After completing the basic processing of the CD43 wave data in May 1991, the analysis of the complete CD43 data set was begun. The results of the analysis were presented in August 1991 at the IUGG in Vienna, where there was a workshop at the end of the session. Toba, the convener of the session, had suggested that all data be presented in a certain format so as to allow easy intercomparison of results. This involved producing plots of non-

dimensionalised roughness length (z_0) against wave age (C_p / $u*$) after the fashion of Toba and Koga (1986). The roughness length was parameterised by $gz_0/u*^2$, and the (inverse) wave age by $2\pi f u*/g$, where f is the frequency of the wind wave peak.

Since Toba's parameterisation was only valid for wind waves in the absence of swell, we split our data into case studies which could be examined separately and concentrated on those where swell was absent. These cases were studied using data from both the Solent sonic and the Kaijo-Denki, with wave data from the SBWR. Wavec data was not used extensively at this point because it was hoped that if the SBWR data proved useful, then the data set could be expanded to include the Cumulus data.

Case study; day 317

The period from day 317.3 to day 318.2 was the clearest example of wind waves only with no swell present. During this period the wind speed increased steadily from 9 to 17 m/s, until 318.0 when it decreased rapidly (Figure 13). The equivalent time series of wave energy spectra from the SBWR is shown in Figure 8. The generation of short wavelength wind waves is seen at the start of the period, with the energy maximum progressing to longer wavelengths with time. This progression of energy is halted and reversed when the wind speed decreases.

Using data from the Solent, the non-dimensionalised roughness vs inverse wave age plot was produced (Figure 14). The data was averaged into hourly periods and classified by eye into periods of increasing winds, steady winds and decreasing winds. In this example a "hysteresis" type curve appears, with periods of increasing winds showing a consistently higher roughness value than the corresponding value for decreasing winds.

However, when the same plot is produced using the data from the Kaijo-Denki anemometer this effect is not seen, Figure 15.

The "hysteresis" type curve does not appear in any other case study even when the Solent sonic is used. In fact, all that can be inferred from this representation of this data is that the roughness length decreases with increasing wave age. This is in opposition to the theory of Toba (1990) but is in agreement with most other researchers results.

Another point of interest is that while friction velocity estimates (Figure 6) from the two different sonics agree well, the agreement for wind speed is

not as good (Figure 5).   This contributes towards the relatively poor agreements between both roughness lengths and drag coefficients (Figures 16 and 17).   This illustrates the difficulty in separating the scatter due to sea state from scatter due to instrumental reasons (e.g. flow disturbance).

3.5 Future Plans

The ultimate goal of this project is to find a parameterisation for sea state and/or changing wind conditions which reduces the present uncertainty in the drag coefficient estimates.   This will involve quantitative determinations of the following;

1) the mean drag coefficients to be expected for different wind speeds for deep water conditions,

2) evaluation of wind stress measurements from a buoy,

3) the proportion of the scatter in drag coefficient which can be explained by varying wave and wind conditions,

4) the relationship between the drag coefficient and sea state.

These stages are discussed in the following sections, along with the strategy to be adopted for the analysis of the different data sets.   Figure 18 summaries the analysis.

3.5.1 Mean drag coefficient

The problem of mean drag coefficient values arises because of the discrepancy between our results from CD43 and those of other researchers; our values are considerably higher than those of Smith (1980) or Large and Pond (1981). In order to asses the size of the discrepancy, it would be useful to know the magnitude of the currents in the area of the other researchers' work.   If this information is not available, or if currents are found which have not been taken into account, then our data can not be compared to theirs.

In order to have confidence in our drag coefficient estimates possible causes of systematic error have to be considered. For example, the air flow may rise significantly over the bow of the ship, resulting in erroneous wind speed estimates.   One way to test this is to use a model of the ship in a wind

tunnel, but this may not be practical. Alternatively, the wind speed measurements taken at different heights (during CD62a) should show whether the wind profile has been disturbed in this way. However, if disturbance of the air flow does prove to be the cause of the discrepancy only the mean drag coefficients will be affected, so the effect of sea state on the stress (i.e. the scatter in the drag coefficients) can still be investigated.

Once drag coefficients have been calculated from CD62a and from the very large Cumulus data set, we should be able to either confirm or explain the CD43 results. If they do prove to be more representative than that from Smith, this will be of importance for ocean modelling, sea wave forecasting and storm surge modelling.

3.5.2 Buoy data evaluation

The data from the new meteorological buoy has yet to be evaluated. By comparing the data from the buoy to similar data from the ship we should be able to tell whether the buoy can be used to provide stress estimates in a routine fashion. The ship comparison of the asymmetric and symmetric head arrangements of the Solent sonics will also be involved here, since the buoy carries the asymmetric version of the anemometer. Trial deployments of the buoy (initially to test the mooring arrangement) will be held later this year. The performance of the buoy may also be tested during a proposed international comparison of dissipation method packages used by various researchers, which may be held under the Commission for Atmospheric Sciences of the WMO.

3.5.3 Drag coefficient scatter

In order to investigate the effects of sea state on wind stress, the causes of scatter in the drag coefficient estimates must be understood. It is generally thought that sea state effects cause some of the scatter, but some will be due to instrumentation or to the measurement method, and these will be investigated first.

Scatter due to the instrumentation is illustrated by the differences in roughness length (Figure 16) produced by two different anemometers, but this may have been caused by slightly different sampling periods. A better understanding of the scatter caused by the anemometers will come from the

investigation of the CD62a data, where two identical Sonics with identical sampling periods were positioned side by side.

Some scatter is probably due to the calculation of the wind speed which relies on the determination of the speed of the ship through the water (discussed in section 3.4.1). This problem will be investigated using data from CD43. Data from the VAESAT buoy will be used to get a time series of current speed and direction, and this, together with the data of the ships speed and direction relative to the ground, should produce information as to the ship's speed through the water. These calculations can than be compared to the data from the em log. If they agree then we will assume the em log information has not been corrupted (by use of the bow thruster) and can be used in the true wind corrections. Periods where the two methods disagree can be investigated further or discounted when looking for wave effects.

Once the causes of experimental scatter are better understood, the investigation into wave effects can begin.

3.5.4 Drag coefficient dependence on sea state

In the investigation of the effects of sea state on stress, two approaches will be tried. The first involves the detailed data sets from the Darwin. When the causes of scatter discussed in the last section have been quantified, the remaining scatter (if any!!) will be related to the wave field data. The best wave field data comes from the Wavec buoy which operated for most of CD43 and produces directional wave spectra up to ~6 Hz. Since the Wavec was not always near to the ship the SBWR will be used for quality control. Additional data may be obtained, if necessary, using the new meteorological buoy which had a first trial during CD62. If the buoy seems satisfactory then it will be used as part of an array, containing a Waverider buoy and a current measuring buoy. These will probably be deployed near-shore during 1993/4. In this way, we should be able to obtain further high quality data sets for evaluating the effects of sea state on the wind stress.

Another use has been proposed for the Darwin data, which could provide some insights to the wave field/ wind stress interaction. Wind speed data from the Darwin will be input to the WAM model, due to be run by POL later this year, and the wave and stress predictions from the model will be compared to the Darwin data.

The second approach to be tried uses the long term data set obtained on the OWS Cumulus. This, more empirical, analysis of the Cumulus data will involve splitting the data into case types; no swell present, swell direction similar to wind direction, swell direction opposing wind, steady wind, increasing wind, decreasing wind, etc. For each of these case types, the drag coefficient/wind speed relation will be produced and analysed for systematic differences. Previous research has generally concentrated on the simplest cases of steady winds with no swell present. If the Cumulus data shows the effect of swell on drag, or the absence of any effect, this should prove very useful. At the very least, drag coefficient values should be obtained under a greater range of wind speeds than has previously been possible.

There is a large backlog of routine processing to be done on all the Cumulus data. The wind speeds have all to be corrected using the scheme outlined in section 3.3.2, and the missing meteorological variables such as sea surface temperature have to be obtained from the Meteorological Office. All the power spectral density data has to be processed and merged with the mean meteorological data before drag coefficient estimates can be produced. The SBWR processing is fairly routine, but information as to the direction of swell has to be obtained from the ship's logs and merged with the other data. Since the Cumulus will probably continue to produce data for the next few years this routine work will be done intermittently over the next two years.

3.6 Summary

Detailed data sets have been collected during the two Darwin cruises, and three years of data has been collected from the Cumulus. A detailed evaluation (Yelland et al., 1991) of the performance of the Solent sonic was produced from the results of cruise CD43, and a paper on the full results from CD43 is being prepared jointly with the researchers from UMIST. Studies of particular events from this data were presented at the 1991 IUGG in Vienna. A new buoy has been developed to obtain stress measurements close to the sea surface, and preliminary data has been collected which will be used to evaluate the buoy's performance. Work done so far has resulted in drag coefficients from the first Darwin cruise (CD43) which are higher than those of other researchers' and these will be compared to the results from both the other Darwin cruise and from the Cumulus data. This work has also

highlighted the importance, and difficulty, of obtaining true wind speed estimates.

References

Charnock, H., 1955: Wind Stress on a Water Surface. *Q. J. Roy. Met. Soc.*, 81, 639-640.

Denman, K. L. and M. Miyake, 1973: Behavior of the Mean Wind, the Drag Coefficient, and the Wave Field in the Open Ocean. *J. Geophys. Res.*, 78(12), 1917-1931.

Donelan, M. A., 1982: The Dependence of the Aerodynamic Drag Coefficient on Wave Parameters. *First International Conference on Meteorology and Air-Sea Interaction of the Coastal Zone*, American Meteorological Society, Boston, Mass., 381-387.

Dyer, A. J., 1974: A review of flux-profile relationships. *Boundary-Layer Meteorol.*, 7, 363-372.

Edson, J. B., C. W. Fairall, P. G. Mestayer and S. E. Larsen, 1991: A Study of the Inertial-Dissipation Method for Computing air-Sea Fluxes. *J. Geophys. Res.*, 96(C6), 10689-10711.

Ewing, J. A., 1986: Presentation and Interpretation of Directional Wave Data. *Underwater Techn.*, 12(3), 17-23.

Garratt, J. R., 1977: Review of Drag Coefficients over Oceans and Continents. *Mon. Wea Rev.*, 105, 915-929.

Geernaert, G., 1990: The Theory and Modeling of Wind Stress with applications to Air-Sea Interaction and Remote Sensing. *Rev. Aquatic Sci.*, 2, 125-149.

Geernaert, G. L., K. L. Davidson, S. E. Larsen and T. Mikkelsen, 1988: Wind Stress Measurements During the Tower Ocean Wave and Radar Dependence Experiment. *J. Geophys. Res.*, 93(C11), 13913-13923.

Geernaert, G. L., K. B. Katsaros and K. Richter, 1986: Variation of the Drag Coefficient and Its Dependence on Sea State. *J. Geophys. Res.*, 91(C6), 7667-7679.

Geernaert, G. L., S. E. Larsen and F. Hansen, 1987: Measurements of the Wind Stress, Heat Flux, and Turbulence Intensity During Storm Conditions Over the North Sea. *J. Geophys. Res.*, 92(C12), 13127-13139.

Graf, W. H., N. Merzi and C. Perrinjaquet, 1984: Aerodynamic Drag Measured at a Nearshore Platform on Lake Geneva. *Arch. Meteorol. Geophys. Bioklimatol. Ser. A*, 33, 151.

Hasse, L., 1986: On Charnock's Relation for the Roughness at Sea. In E. C. Monahan and G. M. Niocaill, Ed.*Ocean Whitecaps*, D. Reidel, pp 49-56.

Hsu, S. A., 1974: A dynamic toughness equation and its application to wind stress determination at the air-sea interface. *J. Phys. Oceanogr.*, 4, 116-120.

Janssen, P. A. E. M., 1989: Wave-induced stress and the drag of air flow over sea waves. *J. Phys. Oceanogr.*, 19, 745-754.

Large, W. G. and J. A. Businger, 1988: A System for Remote Measurements of the Wind Stress over the Oceans. *J. Atmos. & Oceanic Tech.*, 5, 274-285.

Large, W. G. and S. Pond, 1981: Open Ocean Momentum Flux Measurements in Moderate to Strong Winds. *J. Phys. Oceanogr.*, 11, 324-336.

Large, W. G. and S. Pond, 1982: Sensible and Latent Heat Flux Measurements over the Ocean. *J. Phys. Oceanogr.*, 12, 464-482.

Masuda, A. and T. Kusaba, 1987: On the Local Equilibrium of Winds and Wind-waves in Relation to the Surface Drag. *J. Oceanog. Soc. Japan*, 43, 28-36.

Miyake, M., R. W. Stewart, R. W. Burling, L. R. Tsvang, B. M. Koprov and O. M. Kuznetsov, 1971: A Comparison of Acoustic Instruments in the Measurement of Atmospheric Turbulent Flow over Water. *Boundary-Layer Meteorol.*, 2, 228-245.

Roll, H. U., 1965: *Physics of the Marine Atmosphere*, . 7, Academic Press.

Schmitt, K. F., C. A. Friehe and C. H. Gibson, 1978: Sea Surface Stress Measurements. *Boundary-Layer Meteorol.*, 15, 215-228.

Sheppard, P. A., D. T. Tribble and J. R. Garratt, 1972: Studies of turbulence in the surface layer over water (Lough Neagh). I. Instrumentation, programme and profiles. *Q. J. Roy. Met. Soc.*, 948, 627.

Smith, S. D., 1980: Wind Stress and Heat Flux over the Ocean in Gale Force Winds. *J. Phys. Oceanogr.*, 10, 709-726.

Smith, S. D. and E. G. Banke, 1975: Variation of the sea surface drag coefficient with windspeed. *Q. J. Roy. Met. Soc.*, 101, 665.

Stewart, R. W., 1974: The Air-Sea Momentum Exchange. *Boundary-Layer Meteorol.*, 6, 151-167.

Stull, R. B., 1988: *An Introduction to Boundary Layer Meteorology*, .Kluwer Academic Publishers.

Toba, Y., H. Iida, H. Kawamura, N. Ebuchi and I. S. F. Jones, 1990: Wave Dependence of Sea-Surface Wind Stress. *J. Phys. Oceanogr.*, 20, 705-721.

Toba, Y. and M. Koga, 1986: A Parameter Describing Overall Conditions of Wave Breaking, Whitecapping, Sea-Spray Production and Wind Stress. In E. C. Monahan and G. MacNiocaill, Ed., *Oceanic Whitecaps*, Reidel, D., pp 37-47.

Tsvang, L. R., B. M. Koprov, S. L. Zubkovskii, A. J. Dyer, B. B. Hicks, M. Miyake, R. W. Stewart and J. W. McDonald, 1973: A Comparison of Turbulent Measurements by Different Instruments; Tsimlyansk Field Experiment 1970. *Boundary-Layer Meteorol.*, 3, 499-521.

Volkov, Y. A., 1970: Turbulent Flux of Momentum and Heat in the Atmospheric Surface Layer over a Disturbed Sea-Surface. *Izv. Atmos. Oceanic Phys.*, 7, 18-27.

Yelland, M. J., P. K. Taylor, K. G. Birch, R. W. Pascal and A. L. Williams, 1991: *Evaluation of a Solent Sonic Anemometer on RRS Charles Darwin Cruise 43.* 288, Institute of Oceanographical Sciences.
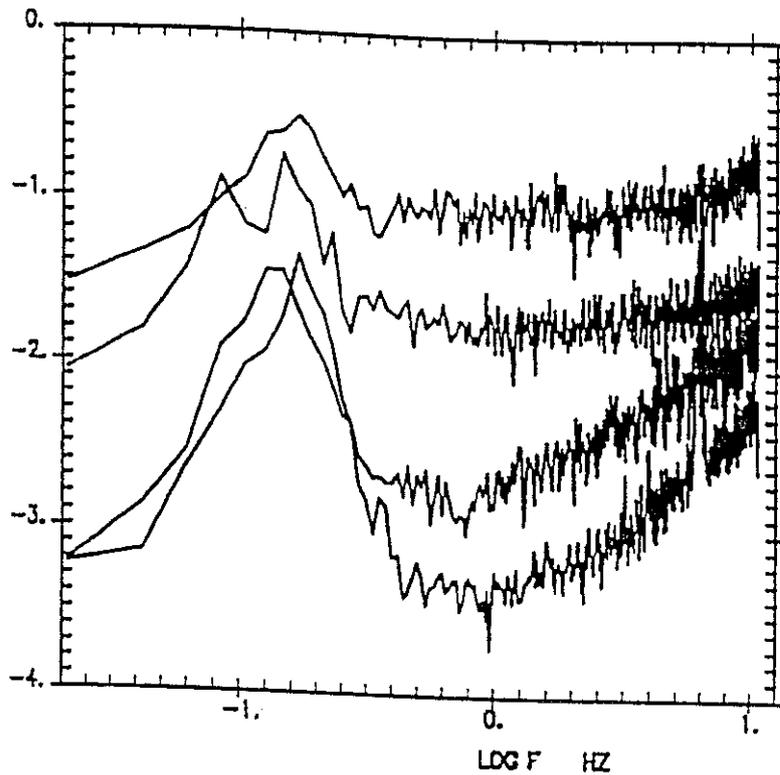
Figure 1   Wind speed spectra obtained at mean wind speeds of, from the top down, 15.5, 10, 3 and 2.5 m/s.   The vertical axis is $\log_{10} (S\ f^{5/3})$, where S is the power spectral density, and the horizontal axis is $\log_{10} f$.
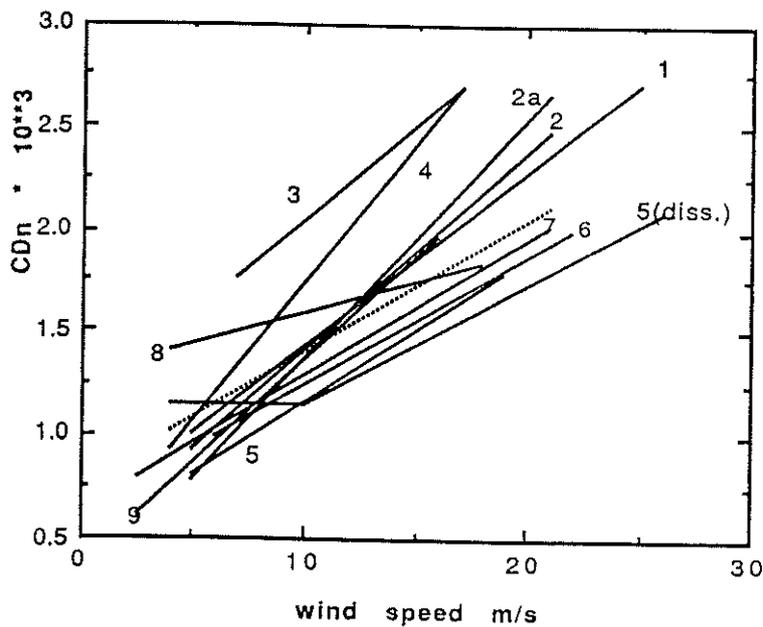

Figure 2   Data reviewed by Garratt (1977) (dotted line) and Geernaert (1990) (solid lines).   The numbers refer to the references in Table 1 of the text; "2a" is the data from Geernaert (1986) where surface currents have been allowed for, and "5diss." is the Large and Pond (1991) data obtained by the dissipation method rather than by the eddy correlation method (line "5" in this figure).
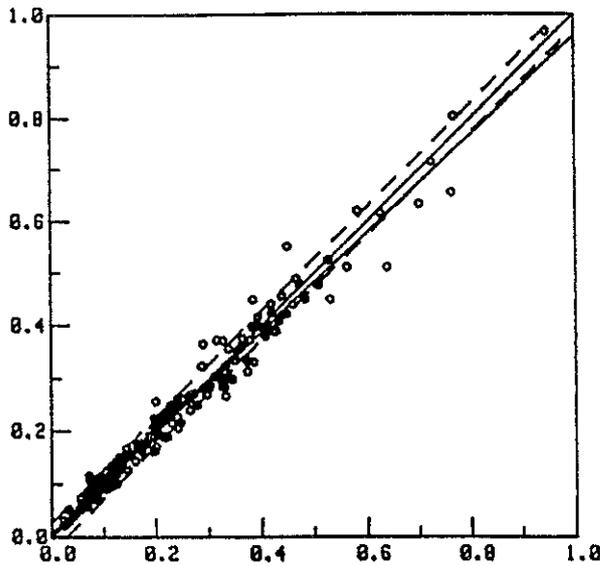
Figure 3   Reproduction of fig.13a from Edson et.al.(1991), showing stress estimates obtained by the dissipation method on the vertical axis (ρu_*2), and from the eddy correlation method on the horizontal axis (-ρ<uw>).
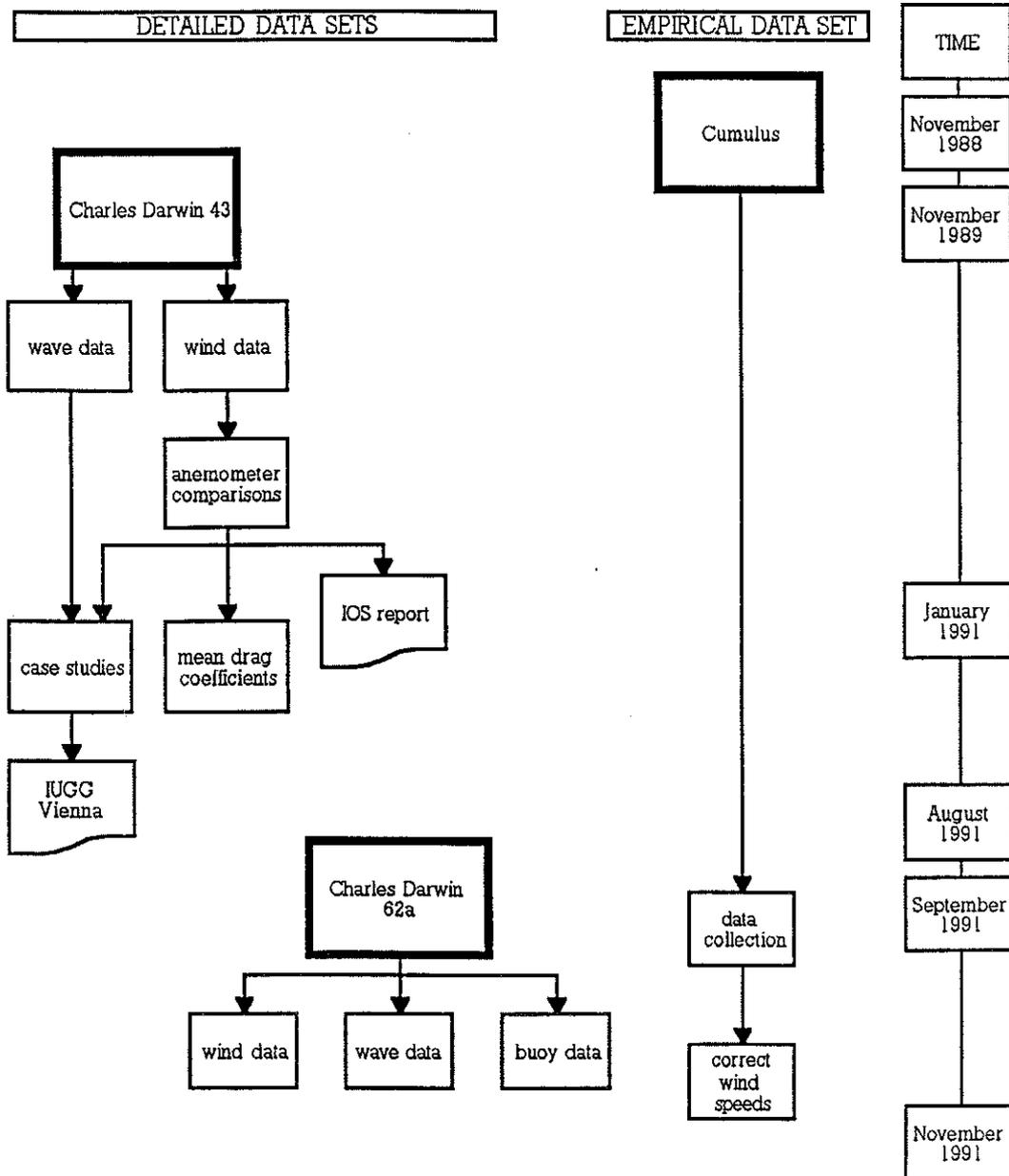
Figure 4   Summary of data collection and processing to date.
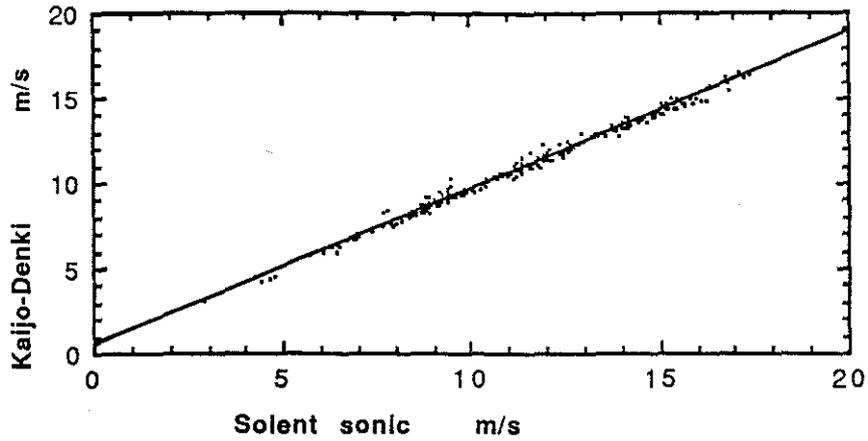
Figure 5   Wind speed data from CD43 for the two different sonic anemometers, with the least squares regression line shown.
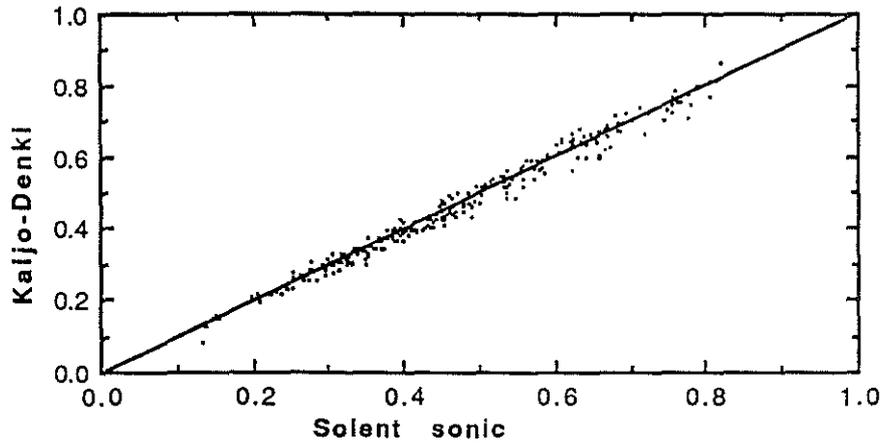
Figure 6   Friction velocity data from CD43 for the two different sonic anemometers, with the least squares regression line shown.
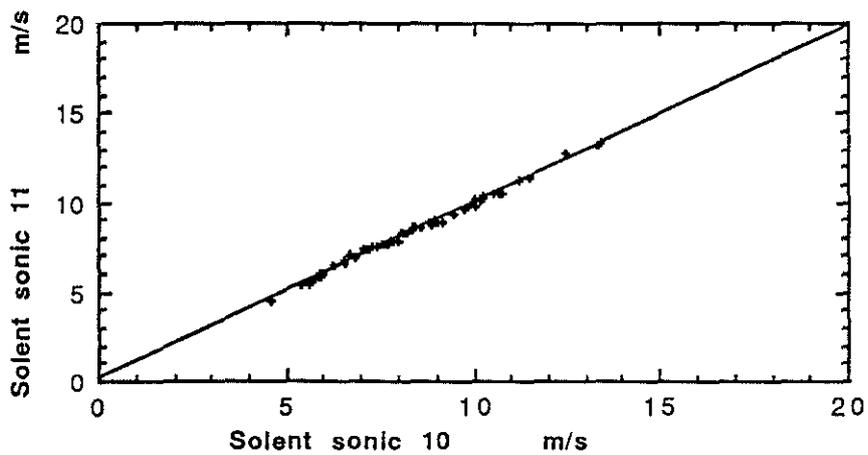
Figure 7   Wind speed comparison for the two Solent sonic anemometers used during CD62a.   The least squares regression is shown.
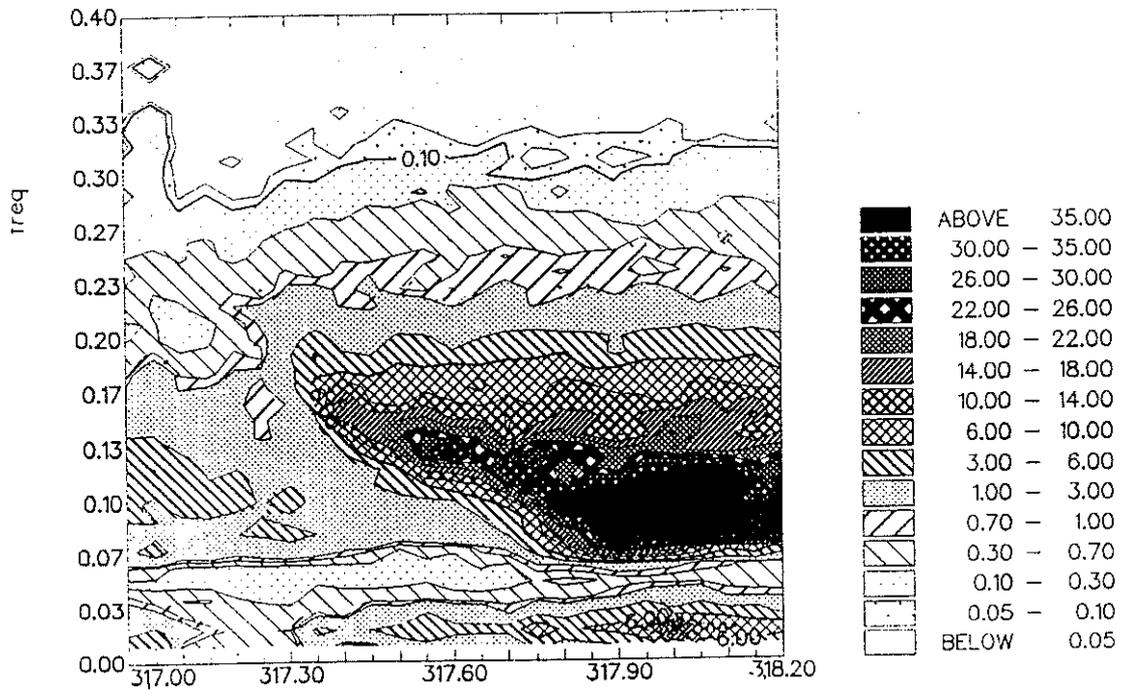
Figure 8   Time series of energy density spectra from the SBWR, covering the period from day 317 to day 318.2.   The vertical axis is frequency (Hz) and the contours show the energy density (m²/Hz).
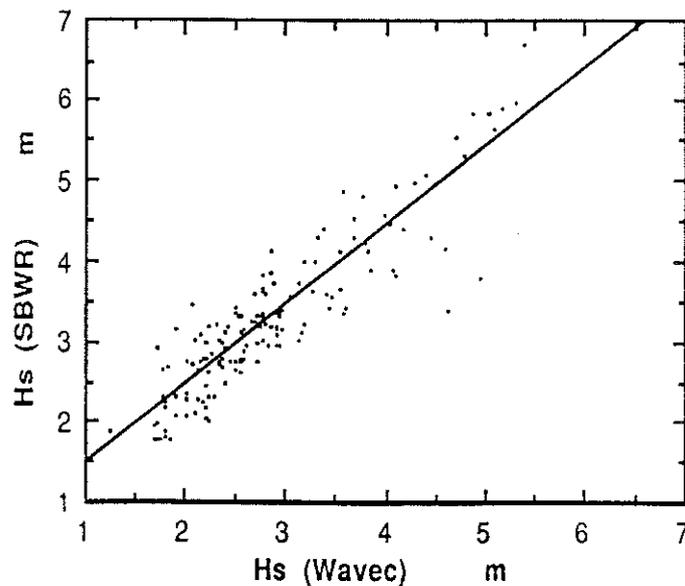
Figure 9   Comparison of significant wave height data from the Ship Borne Wave Recorder (vertical axis) and the WAVEC buoy (horizontal axis).   The least squares regression line is shown.
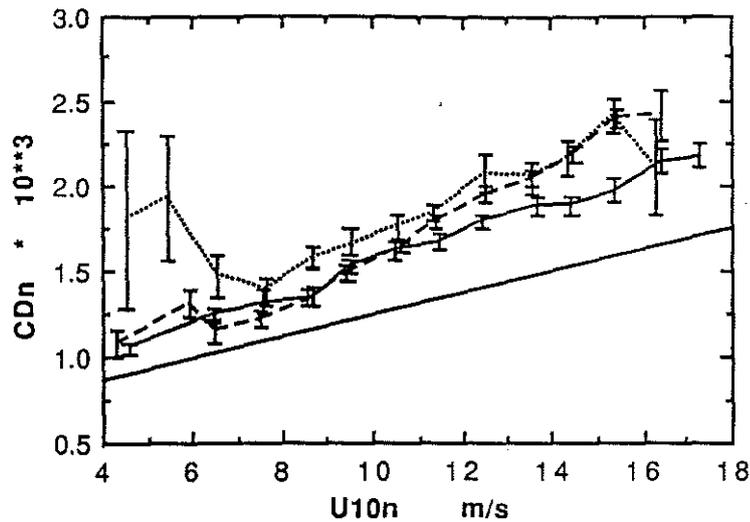
Figure 10   Drag coefficient vs. wind speed relationship from the three anemometers used during CD43; the Solent sonic (solid line), the Kaijo-Denki (dashed line) and the Young (dotted line). Error bars indicate the standard deviation. The Smith (1980) relationship is shown by the straight solid line.
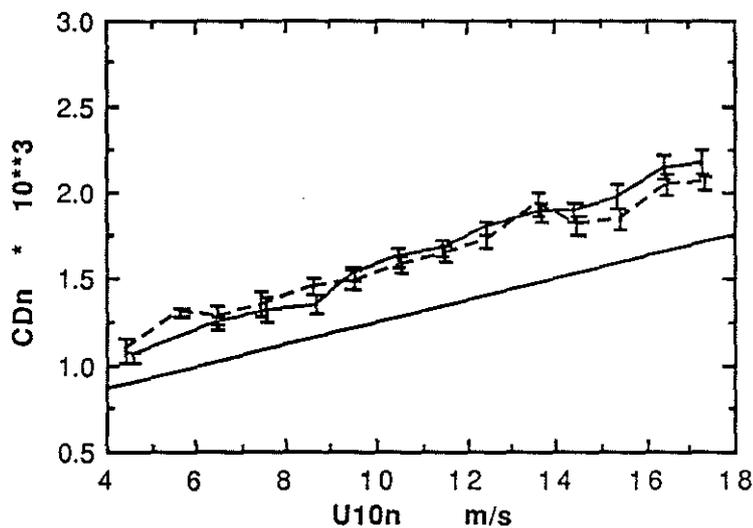
Figure 11   Drag coefficient vs. wind speed relationship from the CD43 Solent sonic data, showing the different methods used to calculate true wind speed; em log (solid line), and ship's speed over the ground (dashed line). The Smith (1980) relationship is indicated by the straight solid line.
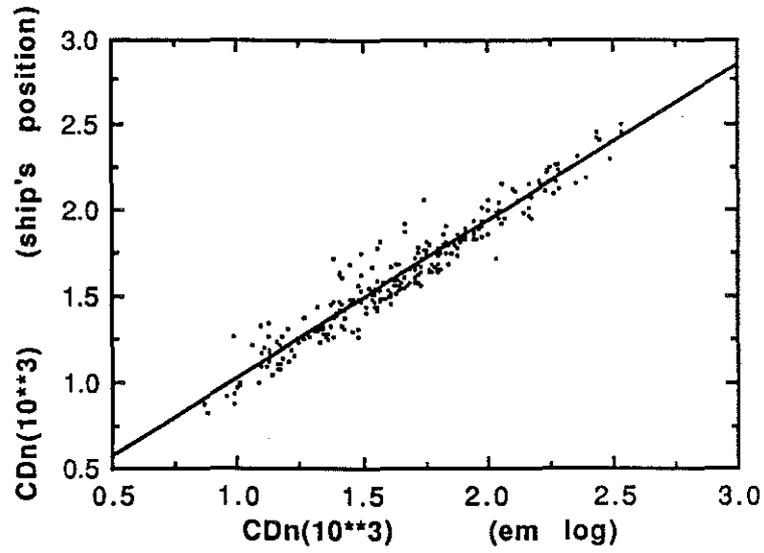
Figure 12   Scatter plot of the drag coefficients calculated using the two different methods of obtaining true wind speed from the same data.   The least squares regression line is shown.
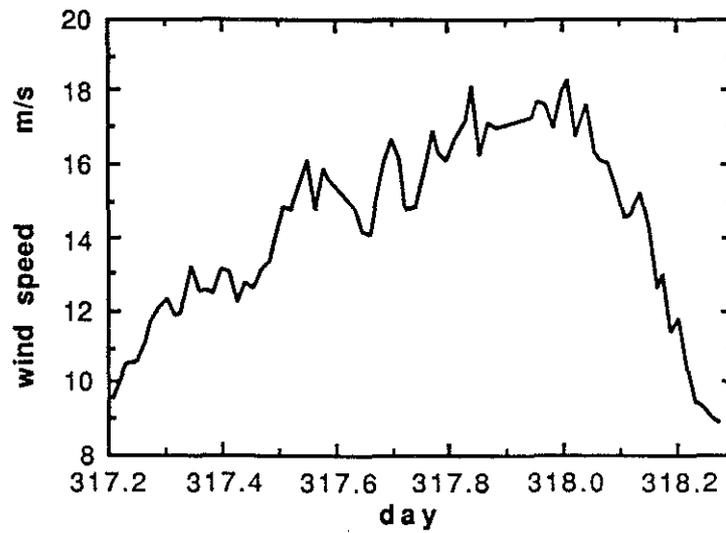
Figure 13   Time series of wind speed for case study "day 317".
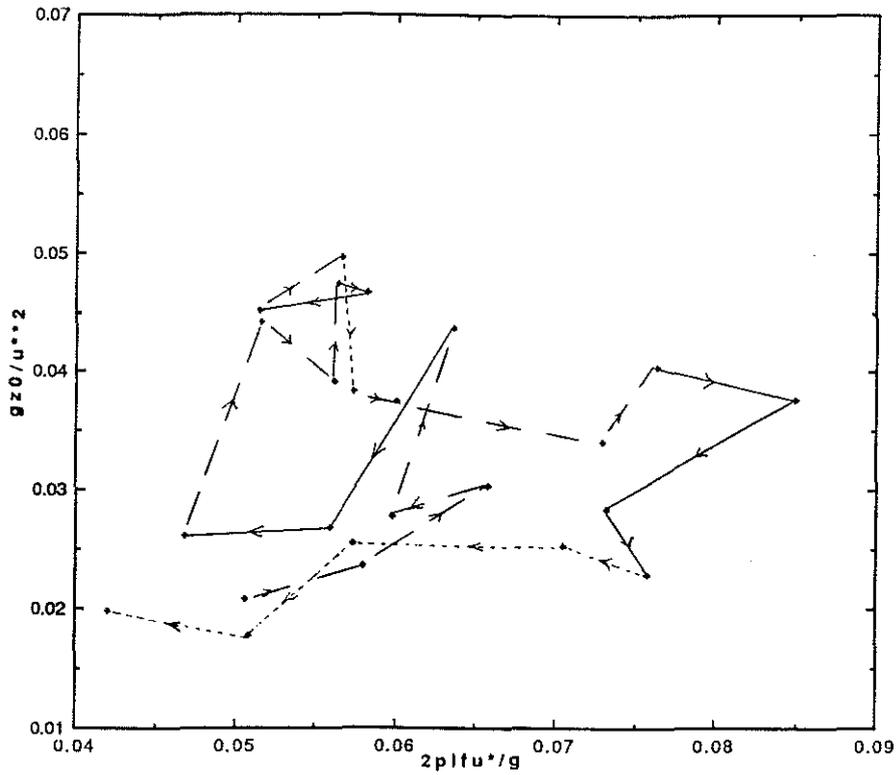
Figure 14   Non-dimensional roughness length against non-dimensional inverse wave age for day 317.   Data from the Solent sonic anemometer is used.   Periods of increasing wind are indicated by a dashed line, steady winds by a solid line and decreasing wind by a dotted line.
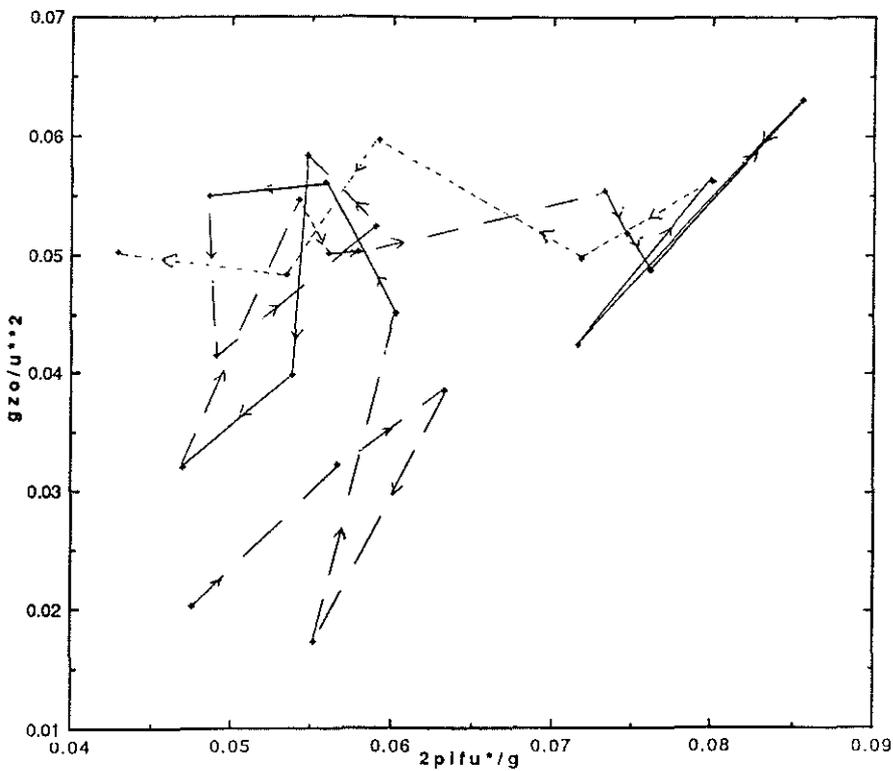
Figure 15   As for Figure 14 but data from the Kaijo-Denki anemometer has been used instead of that from the Solent sonic anemometer.
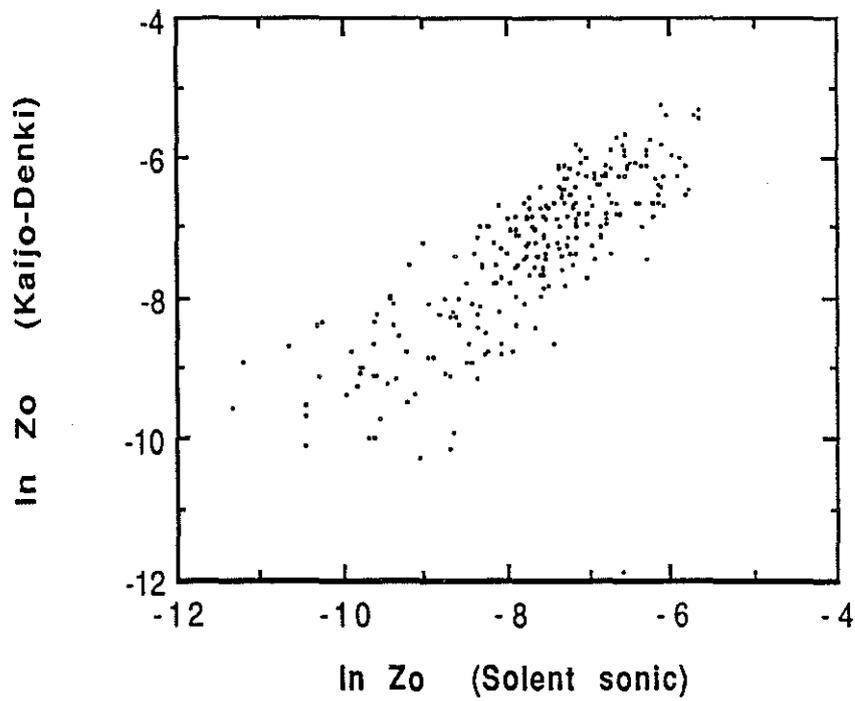
Figure 16   Log$_e$ of the roughness lengths from the two sonic anemometers.
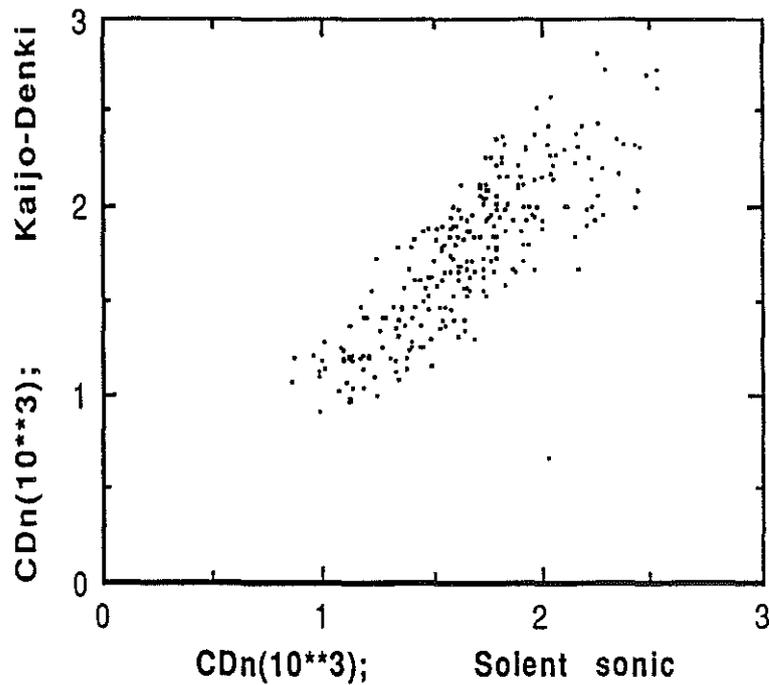

Figure 17   Drag coefficients produced from the Kaijo-Denki anemometer against those from the Solent sonic.
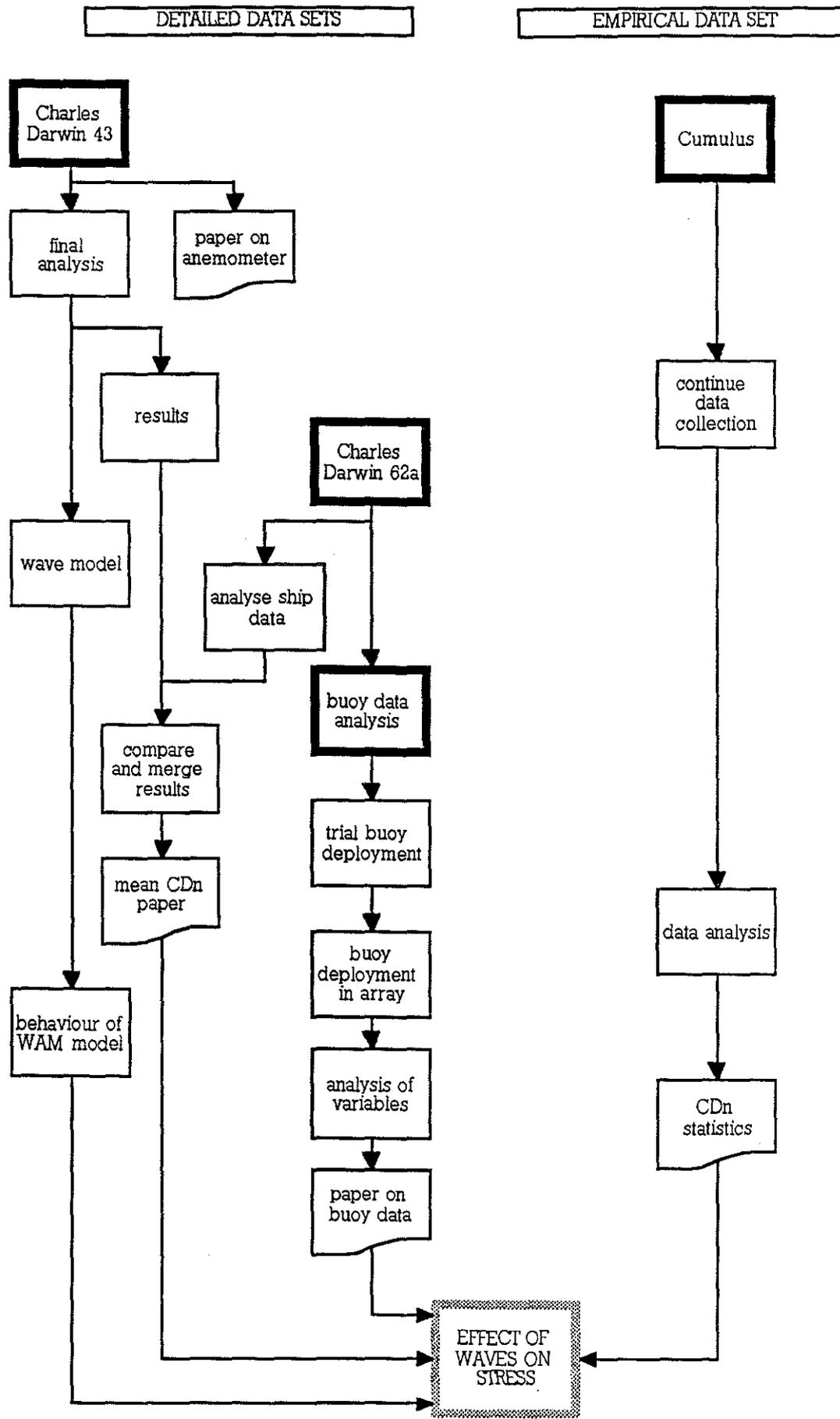
Figure 18   Summary of future work.